Inorganica Chimica Acta 363 (2010) 2848–2856

Contents lists available at ScienceDirect

Inorganica Chimica Acta

journal homepage: www.elsevier.com/locate/ica

Iridium assisted S–H and C–H activation of benzaldehyde thiosemicarbazones. Synthesis, structure and electrochemical properties of the resulting complexes

Semanti Basu [a], Rama Acharyya [a], Falguni Basuli [a], Shie-Ming Peng [b], Gene-Hsiang Lee [b], Golam Mostafa [c], Samaresh Bhattacharya [a,*]

[a] Department of Chemistry, Inorganic Chemistry Section, Jadavpur University, Kolkata 700 032, India
[b] Department of Chemistry, National Taiwan University, Taipei, Taiwan, ROC
[c] Department of Physics, Jadavpur University, Kolkata 700 032, India

ARTICLE INFO

Article history:
Received 22 January 2010
Received in revised form 20 March 2010
Accepted 3 April 2010
Available online 10 April 2010

Dedicated to Prof. Animesh Chakravorty

Keywords:
Benzaldehyde thiosemicarbazones
S–H and C–H activation
Iridium complexes
Coordination modes

ABSTRACT

Reaction of five **4-R**-benzaldehyde thiosemicarbazones (R = OCH_3, CH_3, H, Cl and NO_2) with $[Ir(PPh_3)_3Cl]$ in refluxing ethanol in the presence of a base (NEt_3) affords complexes of three different types, *viz.* **1-R**, **2-R** and **3-R**. In the **1-R** complexes the thiosemicarbazone is coordinated to iridium as a monoanionic bidentate N,S-donor forming a four-membered chelate ring. Two triphenylphosphines, a hydride and a chloride are also coordinated to the metal center. The **2-R** complexes are very similar in composition and stereochemistry to the corresponding **1-R** complexes, except that a second hydride is bound to iridium instead of the chloride. In the **3-R** complexes, the thiosemicarbazones are coordinated to iridium as dianionic tridentate C,N,S-donors forming two adjacent five-membered chelate rings. Two triphenylphosphines and a hydride are also coordinated to the metal center. Structures of the **1-NO_2**, **2-NO_2** and **3-NO_2** complexes have been determined by X-ray crystallography. Reaction of the same **4-R**-benzaldehyde thiosemicarbazones with $[Ir(PPh_3)_3Cl]$ in refluxing toluene in the presence of NEt_3 affords complexes of two types, *viz.* **3-R** and **4-R**. The **4-R** complexes are very similar in composition and stereochemistry to the corresponding **3-R** complexes, except that a chloride is bound to iridium instead of the hydride. Structure of the **4-CH_3** complex has been determined by X-ray crystallography. In all the complexes the two PPh_3 ligands are trans. All the complexes show intense MLCT transitions in the visible region. Cyclic voltammetry on the complexes shows an Ir(**III**)–Ir(**IV**) oxidation on the positive side of SCE followed by an oxidation of the coordinated thiosemicarbazone. A reduction of the coordinated thiosemicarbazone is also observed on the negative side of SCE.

1. Introduction

The chemistry of thiosemicarbazone complexes of the transition metal ions has been receiving significant current attention, largely because of the bioinorganic relevance of these complexes [1]. A large majority of the thiosemicarbazone complexes have found wide medicinal applications owing to their potentially beneficial biological (*viz.* antibacterial, antimalarial, antiviral and antitumor) activities [2]. Systematic studies on the binding of thiosemicarbazones to different transition metal ions are of considerable importance in this respect. However, we have been exploring the chemistry of platinum metal complexes of the thiosemicarbazones [3], with the primary objective of gaining a chemical control over the variable binding mode of these ligands, and the present work has emerged out of this exploration. The aim of the present study has been to scrutinize the interaction of a group of **4-R**-benzaldehyde thiosemicarbazones (**I**) with iridium. It may be relevant to mention here that though the chemistry of thiosemicarbazone complexes of many transition metals has been extensively studied [1], that of iridium appears to have remained practically unexplored [3d]. Upon their reaction with ruthenium and osmium the benzaldehyde thiosemicarbazones (**I**) have been observed to bind to the metal centers, via dissociation of the acidic proton, as monoanionic bidentate N,S-donors forming a rather unusual four-membered chelate ring (**II**) [3a,h–j]. Our investigations have revealed that in view of the geometry of these ligands (**I**) across the C=N bond, formation of the four-membered chelate ring (**II**) is most favorable and that of the five-membered chelate ring (**III**), which appears to be very likely for the thiosemicarbazones in general, is not possible because of the steric hindrance that develops between the phenyl ring of the benzaldehyde thiosemicarbazone and the metal center. It is worth noting here that we have not been able to find a single example of a structurally characterized complex of the benzaldehyde thiosemicarbazones (**I**), where the thiosemicarbazone is coordinated as in **III**. Five-membered chelate ring (**IV**) formation by the benzaldehyde

* Corresponding author.
E-mail address: samaresh_b@hotmail.com (S. Bhattacharya).

0020-1693/$ - see front matter © 2010 Elsevier B.V. All rights reserved.
doi:10.1016/j.ica.2010.04.009

thiosemicarbazones (**I**) has been observed only in very few cases, which are associated with conformational change around the C=N bond [4]. Though five-membered chelate ring (**III**) formation by the benzaldehyde thiosemicarbazones (**I**) without any conformational change has been realized to be impossible, closeness of the phenyl ring to the metal center in **III** points to the possibility of its orthometallation (**V**) via C–H bond activation. Such C–H bond activation is of significant contemporary importance, with particular reference to metal mediated chemical transformations of organic molecules [5]. With the intention of inducing coordination mode **V** in the benzaldehyde thiosemicarbazone ligands (**I**), their reaction has been carried out with a reactive iridium complex, *viz.* $[Ir(PPh_3)_3Cl]$. This particular iridium complex has been chosen as the starting material because of its demonstrated ability to accommodate a tridentate ligand via oxidative addition and, more importantly, its proven efficiency to successfully mediate C–H bond activation of organic molecules [3d,6]. This simple strategy has indeed worked nicely, affording a group of organoiridium complexes, in addition to complexes of other types. This paper deals with the chemistry of all these complexes, with special reference to their formation, structure and electrochemical properties.

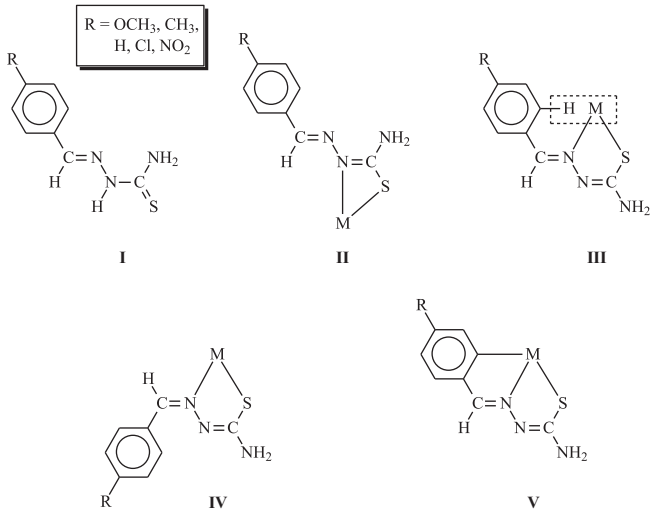

2. Experimental

2.1. Materials

Iridium trichloride was obtained from Arora Matthey, Kolkata, India. $[Ir(PPh_3)_3Cl]$ was prepared as before [6b]. Thiosemicarbazide and the five *para*-substituted benzaldehydes were purchased from SRL, Mumbai, India. The thiosemicarbazone ligands were prepared by reacting equimolar amounts of thiosemicarbazide and the respective *para*-substituted benzaldehyde in 1:1 ethanol–water mixture. Purification of acetonitrile and preparation of tetrabutylammonium perchlorate (TBAP) for electrochemical work were performed as reported in the literature [7]. All other chemicals and solvents were reagent grade commercial materials and were used as received.

2.2. Synthesis

2.2.1. *1*-NO_2, *2*-NO_2 *and* *3*-NO_2

para-Nitrobenzaldehyde thiosemicarbazone (24 mg, 0.10 mmol) was dissolved in ethanol (50 mL) and triethylamine (20 mg, 0.20 mmol) was added to it. The solution was then purged with a stream of dinitrogen for 10 min and to it was added $[Ir(PPh_3)_3Cl]$ (100 mg, 0.10 mmol). The mixture was refluxed under a dinitrogen atmosphere for 24 h, whereby a red solution was obtained. Evaporation of this solution afforded a dark solid, which was subjected to purification by thin layer chromatography on a silica plate. With benzene as the eluant, two distinct red bands separated, which were extracted separately with acetonitrile. Evaporation of the first red fraction gave a 1:1 mixture (in the form of co-crystals) of **1**-NO_2 and **2**-NO_2 (Yield: 42%) and that of the second red fraction afforded **3**-NO_2 (Yield: 25%).

Anal. Calc. for **1**-NO_2 and **2**-NO_2: C, 55.11; H, 4.01; N, 5.84. Found: C, 55.43; H, 4.00; N, 5.88%. ^{1}H NMR [8]: −23.32 (t, hydride, J_{P-H} = 13.5); −20.88 (d of t, hydrides, J_{P-H} = 16.0, J_{H-H} = 7.0); −20.82 (d of t, hydrides, J_{P-H} = 16.0, J_{H-H} = 7.0); 4.63 (s, NH_2); 4.99 (s, NH_2); 7.05 (s, 1H); 7.19 (d, 2H, J_{H-H} = 8.8); 7.21–7.84 (2H + 4PPh_3^*); 7.99 (d, 2H, J_{H-H} = 8.8); 8.04 (d, 2H, J_{H-H} = 8.8); 8.09 (s, 1H). *Anal.* Calc. for **3**-NO_2: C, 56.22; H, 3.94; N, 5.96. Found: C, 56.35; H, 3.92; N, 5.99%. ^{1}H NMR: −14.26 (t, hydride, J_{P-H} = 16.7); 4.46 (s, NH_2); 6.74 (d, 1H, J_{H-H} = 8.3); 7.20–7.62 (1H + 2PPh_3^*); 7.32 (d, 1H, J_{H-H} = 8.1); 7.49 (s, 1H).

2.2.2. *2*-*R* *and* *3*-*R* ($R \neq NO_2$)

All the **2**-**R** and **3**-**R** ($R \neq NO_2$) complexes were synthesized by following the same above procedure using appropriate *para*-substituted benzaldehyde thiosemicarbazone (**I**, $R \neq NO_2$) instead of *para*-nitrobenzaldehyde thiosemicarbazone. A yellow solution was obtained from the synthetic reaction, which afforded a yellow solid upon evaporation. Purification was achieved by thin layer chromatography on a silica plate. With benzene as the eluant, two distinct yellow bands separated, which were extracted separately with acetonitrile. Evaporation of the first yellow fraction gave **2**-**R** (Yield: ∼40%) and that of the second yellow fraction afforded **3**-**R** (Yield: ∼25%).

Anal. Calc. for **2**-OCH_3: C, 58.30; H, 4.53; N, 4.53. Found: C, 58.71; H, 4.47; N, 4.59%. ^{1}H NMR: −20.25 (d of t, hydride, J_{P-H} = 16.0, J_{H-H} = 6.5); −15.80 (d of t, hydride, J_{P-H} = 16.0, J_{H-H} = 6.5); 3.76 (s, OCH_3); 4.48 (s, NH_2); 7.21–7.29 (4H*); 7.30–7.65 (azomethine + 2PPh_3^*). *Anal.* Calc. for **3**-OCH_3: C, 58.43; H, 4.33; N, 4.54. Found: C, 58.91; H, 4.37; N, 4.56%. ^{1}H NMR: −14.50 (t, hydride, J_{P-H} = 16.5); 3.25 (s, OCH_3); 4.25 (s, NH_2); 6.12 (s, 1H); 6.09 (d, 1H, J_{H-H} = 7.4); 6.63 (d, 1H, J_{H-H} = 7.5); 6.81 (s, azomethine); 7.13–7.75 (2PPh_3^*).

Anal. Calc. for **2**-CH_3: C, 59.33; H, 4.61; N, 4.61. Found: C, 59.82; H, 4.53; N, 4.67%. ^{1}H NMR: −19.33 (d of t, hydride, J_{P-H} = 16.5, J_{H-H} = 6.0); −15.27 (d of t, hydride, J_{P-H} = 16.5, J_{H-H} = 6.0); 1.99 (s, CH_3); 4.49 (s, NH_2); 7.05–7.15 (4H*); 7.29–7.66 (azomethine + 2PPh_3^*). *Anal.* Calc. for **3**-CH_3: C, 59.46; H, 4.40; N, 4.62. Found: C, 60.02; H, 4.44; N, 4.67%. ^{1}H NMR: −14.21 (t, hydride, J_{P-H} = 16.5); 1.78 (s, CH_3); 4.61 (s, NH_2); 6.52 (s, 1H); 6.65 (d, 1H, J_{H-H} = 7.4); 6.96 (s, azomethine); 7.02 (d, 1H, J_{H-H} = 8.2); 7.12–7.58 (2PPh_3^*).

Anal. Calc. for **2**-**H**: C, 58.92; H, 4.46; N, 4.69. Found: C, 59.37; H, 4.41; N, 4.62%. ^{1}H NMR: −19.31 (d of t, hydride, J_{P-H} = 18.0, J_{H-H} = 6.0); −15.28 (d of t, hydride, J_{P-H} = 16.5; J_{H-H} = 6.0); 4.55 (s, NH_2); 7.07–7.11 (3H*); 7.13–7.16 (2H*); 7.18–7.68 (azomethine + 2PPh_3^*). *Anal.* Calc. for **3**-**H**: C, 59.05; H, 4.25; N, 4.70. Found: C, 59.39; H, 4.23; N, 4.69%. ^{1}H NMR: −14.48 (t, hydride, J_{P-H} = 18.0); 4.26 (s, NH_2); 6.05 (t, 1H, J_{H-H} = 7.0); 6.43 (t, 1H, J_{H-H} = 7.3); 6.59 (d, 1H, J_{H-H} = 7.3); 6.64 (d, 1H, J_{H-H} = 7.3); 6.71 (s, azomethine); 7.05–7.69 (2PPh_3^*).

Anal. Calc. for **2**-**Cl**: C, 56.73; H, 4.19; N, 4.51. Found: C, 57.11; H, 4.22; N, 4.55%. ^{1}H NMR: −19.27 (d of t, hydride, J_{P-H} = 16.5, J_{H-H} = 6.0); −15.34 (d of t, hydride, J_{P-H} = 18.0; J_{H-H} = 6.0); 4.58 (s, NH_2); 7.05 (d, 2H, J_{H-H} = 8.0); 7.16 (d, 2H, J_{H-H} = 8.5); 7.20–7.67 (azomethine + 2PPh_3^*). *Anal.* Calc. for **3**-**Cl**: C, 56.85; H, 3.98; N, 4.52. Found: C, 57.29; H, 3.92; N, 4.56%. ^{1}H NMR: −14.49 (t, hydride, J_{P-H} = 18.0); 4.30 (s, NH_2); 6.46 (d, 1H, J_{H-H} = 8.0); 6.51 (s,

1H); 6.63 (d, 1H, J_{H-H} = 8.0); 6.90 (s, azomethine); 7.15–7.68 (2PPh$_3^*$).

2.2.3. 4-R

All the **4-R** complexes were synthesized by following a general procedure. Specific details for a particular complex, viz. **4-OCH$_3$**, are given below.

para-Methoxybenzaldehyde thiosemicarbazone (21 mg, 0.10 mmol) was dissolved in toluene (50 mL) and triethylamine (20 mg, 0.20 mmol) was added to it. The solution was then purged with a stream of dinitrogen for 10 min and to it was added [Ir(PPh$_3$)$_3$Cl] (100 mg, 0.10 mmol). The mixture was refluxed under a dinitrogen atmosphere for 24 h, whereby a yellow solution was obtained. Evaporation of this solution afforded a dark solid, which was purified by thin layer chromatography on a silica plate. With benzene as the eluant, two yellow bands separated, which were extracted separately with acetonitrile. Slow evaporation of the first yellow extract afforded the **4-OCH$_3$** complex (Yield: 45%) and that of the second yellow extract afforded the **3-OCH$_3$** complex (Yield: 30%).

Anal. Calc. for **4-OCH$_3$**: C, 56.33; H, 4.07; N, 4.38. Found: C, 56.59; H, 4.10; N, 4.41%. ^{1}H NMR: 3.43 (OCH$_3$); 4.32 (s, NH$_2$); 6.40 (d, 1H, J_{H-H} = 8.5); 6.59 (s, 1H); 6.69 (s, azomethine); 6.89 (d, 1H, J_{H-H} = 8.1); 7.15–7.6 (2PPh$_3^*$). *Anal*. Calc. for **4-CH$_3$**: C, 57.28; H, 4.14; N, 4.45. Found: C, 57.54; H, 4.09; N, 4.47%. ^{1}H NMR: 2.00 (CH$_3$); 4.60 (s, NH$_2$); 6.57 (d, 1H, J_{H-H} = 7.6); 6.80 (s, 1H); 6.84 (d, 1H, J_{H-H} = 7.9); 6.90 (s, azomethine); 7.18–7.55 (2PPh$_3^*$). *Anal*. Calc. for **4-H**: C, 56.85; H, 3.98; N, 4.52. Found: C, 57.04; H, 3.99; N, 4.55%. ^{1}H NMR: 4.31 (s, NH$_2$); 6.51 (t, 1H, J_{H-H} = 7.3); 6.67 (s, azomethine); 6.74 (t, 1H, J_{H-H} = 7.2); 6.90 (d, 1H, J_{H-H} = 7.4); 7.14–7.70 (1H + 2PPh$_3^*$). *Anal*. Calc. for **4-Cl**: C, 54.82; H, 3.74; N, 4.36. Found: C, 55.13; H, 3.80; N, 4.39%. ^{1}H NMR: 4.51 (s, NH$_2$); 6.71 (d, 1H, J_{H-H} = 8.2); 6.84 (d, 1H, J_{H-H} = 7.9); 7.06 (s, 1H); 7.19 (s, azomethine); 7.20–7.56 (2PPh$_3^*$). *Anal*. Calc. for **4-NO$_2$**: C, 54.22; H, 3.69; N, 5.75. Found: C, 54.68; H, 3.73; N, 5.76%. ^{1}H NMR: 4.48 (s, NH$_2$); 6.91 (s, azomethine); 6.97 (d, 1H, J_{H-H} = 7.9); 7.18–7.86 (1H + 2PPh$_3^*$); 8.02 (s, 1H).

2.3. Physical measurements

Microanalyses (C, H, N) were performed using a Heraeus Carlo Erba 1108 elemental analyzer. IR spectra were obtained on a Perkin–Elmer 783 spectrometer with samples prepared as KBr pellets. Electronic spectra were recorded on a JASCO V-570 spectrophotometer. ^{1}H NMR spectra were recorded in CDCl$_3$ solution on a Bruker Avance DPX 300 NMR spectrometer using TMS as the internal standard. Electrochemical measurements were made using a CH Instruments model 600A electrochemical analyzer. A platinum disk working electrode, a platinum wire auxiliary electrode and an aqueous saturated calomel reference electrode (SCE) were used in the cyclic voltammetry experiments. All electrochemical experiments were performed under a dinitrogen atmosphere. All electrochemical data were collected at 298 K and are uncorrected for junction potentials.

2.4. Crystallography

Single crystals of the **1-NO$_2$** + **2-NO$_2$**, and **3-NO$_2$** complexes were obtained by slow evaporation of 1:1 dichloromethane-acetonitrile solutions of the respective complexes. Single crystals of the **4-CH$_3$** complex were obtained by slow diffusion of toluene into an acetonitrile solution of the complex. Selected crystal data and data collection parameters are given in Table 1. Data on the crystals of the **1-NO$_2$** + **2-NO$_2$**, and **4-CH$_3$** complexes were collected on a Bruker Smart CCD diffractometer, while those on the crystal of the **3-NO$_2$** complex were collected on a Nonius CAD4 diffractometer. X-ray data reduction and, structure solution and refinement were done using SHELXS-97 and SHELXL-97 programs [9]. The structures were solved by direct methods.

3. Results and discussion

3.1. Syntheses and crystal structures

Five **4-R**-benzaldehyde thiosemicarbazones (**I**) have been used in the present study, differing in the inductive effect of the substituent R (R = OCH$_3$, CH$_3$, H, Cl, and NO$_2$), in order to observe their influence, if any, on the redox potentials of the complexes. Reactions of the selected thiosemicarbazones (**I**) with [Ir(PPh$_3$)$_3$Cl] proceed smoothly in refluxing ethanol in the presence of triethylamine and each of these reactions affords two products. From the reaction with the *para*-nitrobenzaldehyde thiosemicarbazone two red products are obtained, whereas reaction with each of

Table 1
Crystallographic data for the **1-NO$_2$**, **2-NO$_2$**, **3-NO$_2$** and **4-CH$_3$** complexes.

	1-NO$_2$ + **2-NO$_2$**·CH$_3$CN	**3-NO$_2$**·$^1/_2$H$_2$O	**4-CH$_3$**·C$_6$H$_5$CH$_3$
Empirical formula	$C_{45}H_{40}N_{4.50}O_2P_2SCl_{0.50}Ir$	$C_{44}H_{38}N_4O_{2.50}P_2SIr$	2($C_{45}H_{39}N_3P_2SClIr$), C_7H_8
Formula weight	979.74	948.98	1979.08
Crystal system	orthorombic	triclinic	triclinic
Space group	*P*nma	$P\bar{1}$	$P\bar{1}$
a (Å)	21.5655(4)	12.293(3)	12.219(8)
b (Å)	14.9787	19.760(4)	17.699(11)
c (Å)	27.5334(5)	20.014(4)	21.642(14)
α (°)	90	90.02(3)	74.577(14)
β (°)	90	98.60(3)	87.688(14)
γ (°)	90	106.97(3)	80.750(14)
V (Å^3)	8893.9(3)	4592.7(16)	4453(5)
Z	8	4	2
λ (Å)	0.71073	0.71073	0.71073
Crystal size (mm^3)	0.33 × 0.25 × 0.10	0.50 × 0.40 × 0.30	0.32 × 0.24 × 0.12
T (K)	295(2)	295(2)	100(2)
μ (mm^{-1})	3.192	3.061	3.213
R_1[a]	0.0646	0.0419	0.0641
wR_2[b]	0.1592	0.1312	0.1349
GOF[c]	1.002	1.091	1.00

[a] $R_1 = \Sigma||F_o| - |F_c||/\Sigma|F_o|$.
[b] $wR_2 = [\Sigma\{w(F_o^2 - F_c^2)^2\}/\Sigma\{w(F_o^2)\}]^{1/2}$.
[c] GOF = $[\Sigma(w(F_o^2 - F_c^2)^2)/(M - N)]^{1/2}$, where *M* is the number of reflections and *N* is the number of parameters refined.

the other four thiosemicarbazones (with R≠NO_2) yields two yellow products. Structures of the two red products obtained from the reaction with the *para*-nitrobenzaldehyde thiosemicarbazone have been determined by X-ray crystallography. The structure of the first red product [10] reveals it to be a 1:1 mixture of two complexes, henceforth referred to as complexes **1-NO_2** and **2-NO_2**. Structures of the individual **1-NO_2** and **2-NO_2** complexes are displayed, respectively in Figs. 1 and 2, and some relevant bond parameters are listed in Table 2. In the **1-NO_2** complex (Fig. 1) the thiosemicarbazone is coordinated to iridium, via loss of the acidic proton, as a bidentate N,S-donor forming a four-membered chelate ring (**II**). Two triphenylphosphines, a hydride and a chloride are also coordinated to the metal center. Iridium is thus sitting in a HNP_2SCl coordination sphere, which is distorted considerably from ideal octahedral geometry. The coordinated thiosemicarbazone, hydride and chloride have constituted one equatorial plane with the metal at the center, where the chloride is trans to the sulfur and the hydride is trans to the nitrogen. The PPh_3 ligands have taken up the remaining two axial positions and hence they are mutually trans. The Ir–N distance is a bit longer than usual, probably due to the strong trans influence of the hydride. The other bond distances around the metal center and within the chelated thiosemicarbazone are all quite normal [6,11]. Structure of the **2-NO_2** complex (Fig. 2) is very similar to that of the **1-NO_2** complex, except that a second hydride is coordinated to iridium instead of the chloride. The Ir-S bond is significantly longer than that in the **1-NO_2** complex, and the observed elongation may be attributed again to the trans influence of the hydride. The other bond parameters are comparable to those in the **1-NO_2**.

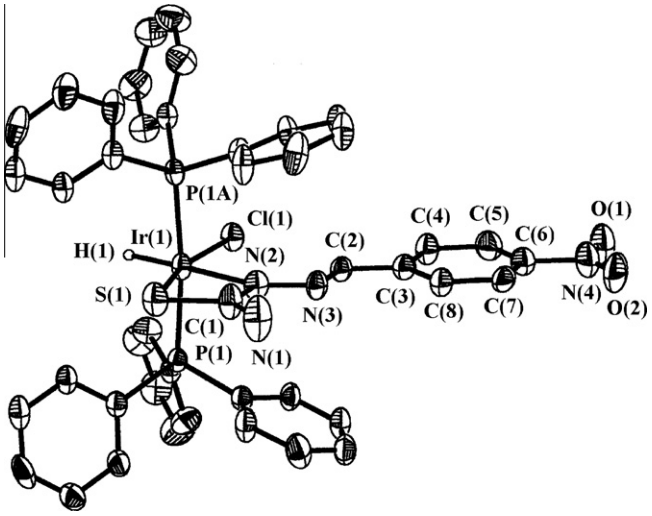

Fig. 1. View of the **1-NO_2** complex.

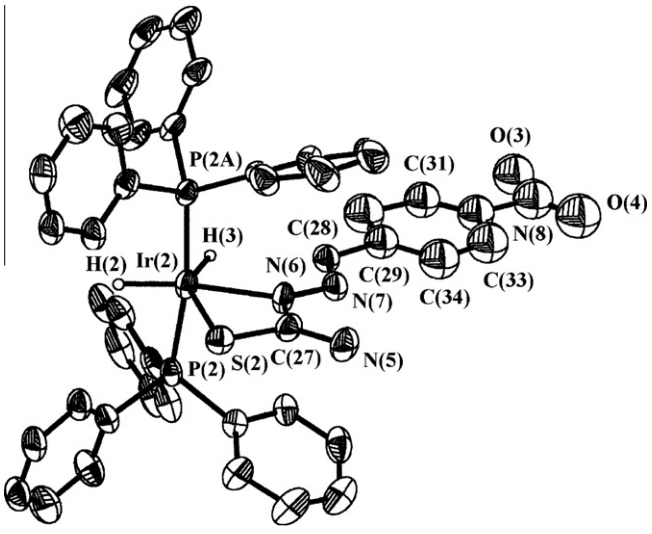

Fig. 2. View of the **2-NO_2** complex.

Table 2
Selected bond lengths (Å) and bond angles (°) for **1-NO_2**, **2-NO_2**, **3-NO_2** and **4-CH_3** complexes.

1-NO_2			
Bond lengths (Å)			
Ir(1)–H(1)	1.497(10)	Ir(1)–Cl(1)	2.409(3)
Ir(1)–N(2)	2.206(9)	C(1)–N(2)	1.278(15)
Ir(1)–P(1)	2.334(2)	C(2)–N(3)	1.256(14)
Ir(1)–P(1A)	2.334(2)	N(2)–N(3)	1.393(13)
Ir(1)–S(1)	2.379(3)	C(1)–S(1)	1.732(13)
Bond angles (°)			
H(1)–Ir(1)–N(2) 177(4)		S(1)–Ir(1)–Cl(1) 165.10(12)	
P(1)–Ir(1)–P(1A) 173.80(9)		N(2)–Ir(1)–S(1) 65.5(3)	
2-NO_2			
Bond lengths (Å)			
Ir(2)–H(2)	1.504(10)	Ir(2)–S(2)	2.521(3)
Ir(2)–H(3)	1.496(10)	C(27)–N(6)	1.326(17)
Ir(2)–N(6)	2.142(10)	C(28)–N(7)	1.268(17)
Ir(2)–P(2)	2.281(3)	N(6)–N(7)	1.337(14)
Ir(2)–P(2A)	2.281(3)	C(27)–S(2)	1.693(15)
Bond angles (°)			
H(2)–Ir(2)–N(6) 164(5)		P(2)–Ir(2)–P(2A) 171.37(10)	
H(3)–Ir(2)–S(2) 143(5)		N(6)–Ir(2)–S(2) 64.7(3)	
3-NO_2			
Bond lengths (Å)			
Ir(1)–H(1)	1.41(2)	Ir(1)–S(1)	2.424(2)
Ir(1)–C(8)	2.042(8)	C(1)–N(2)	1.290(11)
Ir(1)–N(3)	2.073(7)	C(2)–N(3)	1.301(11)
Ir(1)–P(1)	2.302(2)	N(2)–N(3)	1.351(9)
Ir(1)–P(2)	2.305(2)	C(1)–S(1)	1.738(9)
Bond angles (°)			
H(1)–Ir(1)–N(3) 175(4)		C(8)–Ir(1)–N(3) 80.3(3)	
C(8)–Ir(1)–S(1) 159.7(2)		N(3)–Ir(1)–S(1) 79.5(2)	
P(1)–Ir(1)–P(2) 165.43(8)			
4-CH_3			
Bond lengths (Å)			
Ir(1)–N(1)	2.006(7)	Ir(1)–Cl(1)	2.389(3)
Ir(1)–S(1)	2.433(3)	N(1)–N(2)	1.462(10)
Ir(1)–C(1)	2.013(9)	C(7)–N(1)	1.302(11)
Ir(1)–P(1)	2.346(3)	C(8)–N(2)	1.317(11)
Ir(1)–P(2)	2.367(3)	C(8)-S(1)	1.745(9)
Bond angles (°)			
C(1)–Ir(1)–S(1) 160.4(2)		C(1)–Ir(1)–N(1) 79.4(3)	
N(1)–Ir(1)–Cl(1) 173.7(2)		N(1)–Ir(1)–S(1) 81.1(2)	
P(1)–Ir(1)–P(2) 169.53(8)			

The second red product [10] has been found to be a single complex, henceforth referred to as complex **3-NO_2**, and its structure is shown in Fig. 3. In this complex the thiosemicarbazone is coordinated to iridium as a tridentate C,N,S-donor (**V**) via loss of two protons. Two triphenylphosphines and a hydride are also coordinated to iridium. The tricoordinated thiosemicarbazone ligand is sharing the same equatorial plane with iridium and the hydride, and the PPh_3 ligands are trans as before. The Ir–C distance is normal [6], and the other bond distances (Table 2) within the iridium-bound thiosemicarbazone fragment are consistent with the bond descriptions shown in **V**.

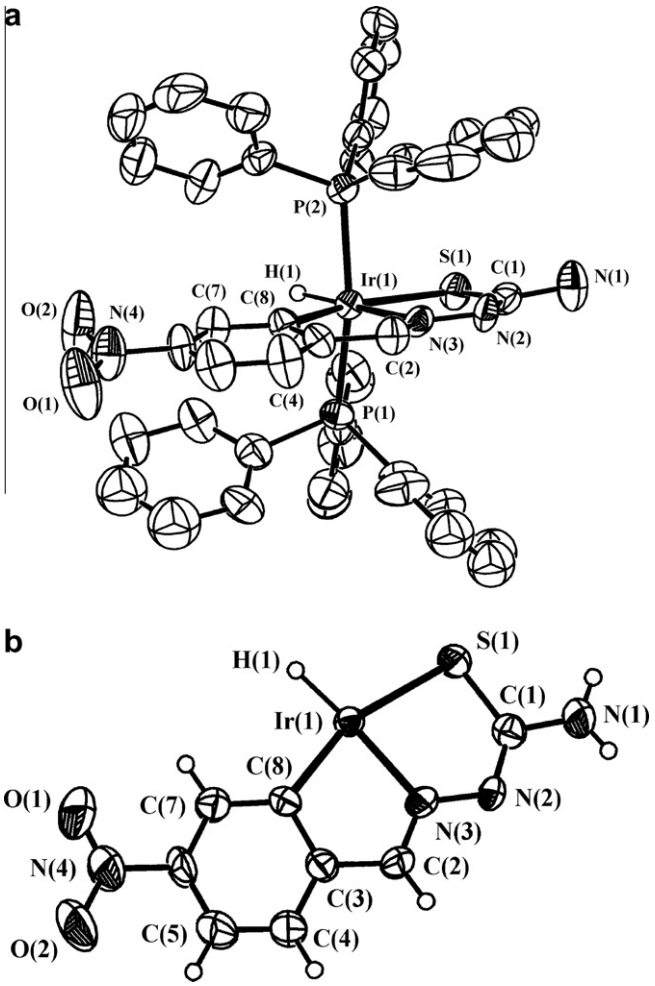

Fig. 3. View of (a) the **3-NO$_2$** complex and (b) the equatorial plane in it.

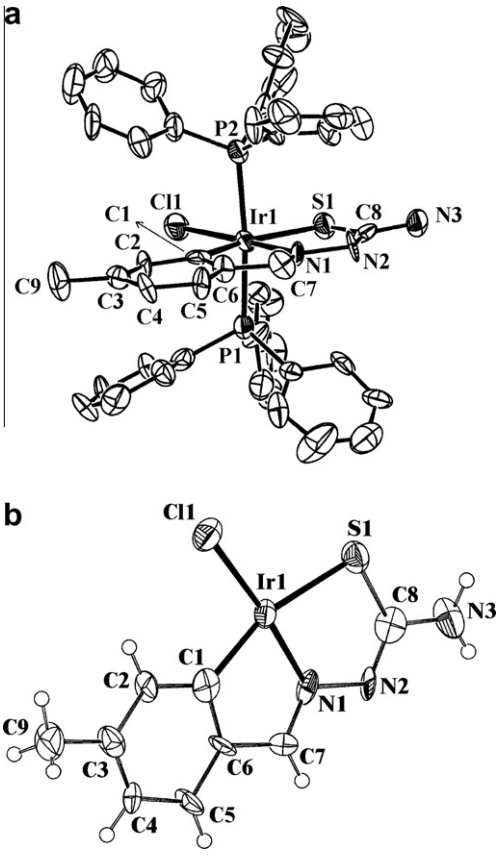

Fig. 4. View of (a) the **4-CH$_3$** complex and (b) the equatorial plane in it.

The first group of yellow complexes [12], obtained from reactions with the four thiosemicarbazones with R≠NO$_2$, are found to have composition similar to that of the **2-NO$_2$** complex, and they show similar spectral and electrochemical properties as the **2-NO$_2$** complex (*vide infra*). Hence these yellow complexes are assumed to have similar structures as the **2-NO$_2$** complex. These four yellow complexes, along with the **2-NO$_2$** complex, are in general referred to as the **2-R** complexes. The second group of yellow complexes [12] are found to be similar, in composition and properties, to the **3-NO$_2$** complex, and so they are assumed to have similar structures as the **3-NO$_2$** complex. These second group of yellow complexes, along with the **3-NO$_2$** complex, are in general referred to as the **3-R** complexes.

The presence of hydride in all the above complexes has been quite intriguing. Two sources of the hydride seem probable. Oxidative addition of iridium(**I**) to the thiosemicarbazone may generate a hydride out of the acidic proton, or the solvent (ethanol) may serve as a source of the hydride. To check this, reactions of the **4-R**-benzaldehyde thiosemicarbazones (**I**) with [Ir(PPh$_3$)$_3$Cl] have also been carried out in a non-alcoholic solvent, viz. toluene, in the presence of triethylamine. Each of these reactions has afforded complexes of two types, one of which has been found to be the same **3-R** complex obtained from the ethanol reaction. This clearly indicates that ethanol has not been the only source of hydride in these **3-R** complexes. Preliminary characterizations (viz. microanalysis, IR and ^{1}H NMR) on the complexes of the second type, henceforth referred to as the **4-R** complexes, show that they are very similar to the corresponding **3-R** complexes except that a chloride is bound to iridium instead of the hydride. Further authentication has been done by structure determination of a representative complex from this family, viz. **4-CH$_3$**, which shows (Fig. 4, Table 2) that the benzaldehyde thiosemicarbazone is coordinated to iridium as a tridentate C,N,S-donor (**V**) and, two triphenylphosphines and a chloride are also coordinated to the metal center. The Ir–Cl bond length is normal and the other structural features compare well with those of the **3-NO$_2$** complex. As all the five **4-R** complexes have been synthesized similarly and they show similar properties (*vide infra*), the other four members of this group (with R≠CH$_3$) are assumed to have a similar structure as the **4-CH$_3$** complex.

The synthetic reactions carried out in two different solvents show that the nature of products obtained depends on the nature of solvent used. When ethanol is used as the solvent, complexes of three types, viz. **1-R** (R = NO$_2$), **2-R** and **3-R**, are obtained. The mechanism behind formation of these three types of complexes is not completely clear to us. However, the sequences shown in Scheme 1 seem probable. The synthetic reaction seems to have proceeded by following two different kinetic routes. In one route, oxidative insertion of iridium into the S-H bond (in the thiolate tautomer) takes place in the initial step associated with simultaneous dissociation of one PPh$_3$, and thus the thiosemicarbazone binds to the metal center as a bidentate N,S-donor forming a four-membered chelate ring (**II**) and affords the **1-R** complex. Precedence of such S–H activation is available in the literature [13]. This particular complex could be trapped only for the R = NO$_2$ case. The **1-R** complex then reacts with ethanol in the presence of NEt$_3$, whereby the coordinated chloride got displaced by a hydride, and thus the corresponding dihydride complex **2-R** is produced. Formation of such iridium hydride from a chloride precursor is well

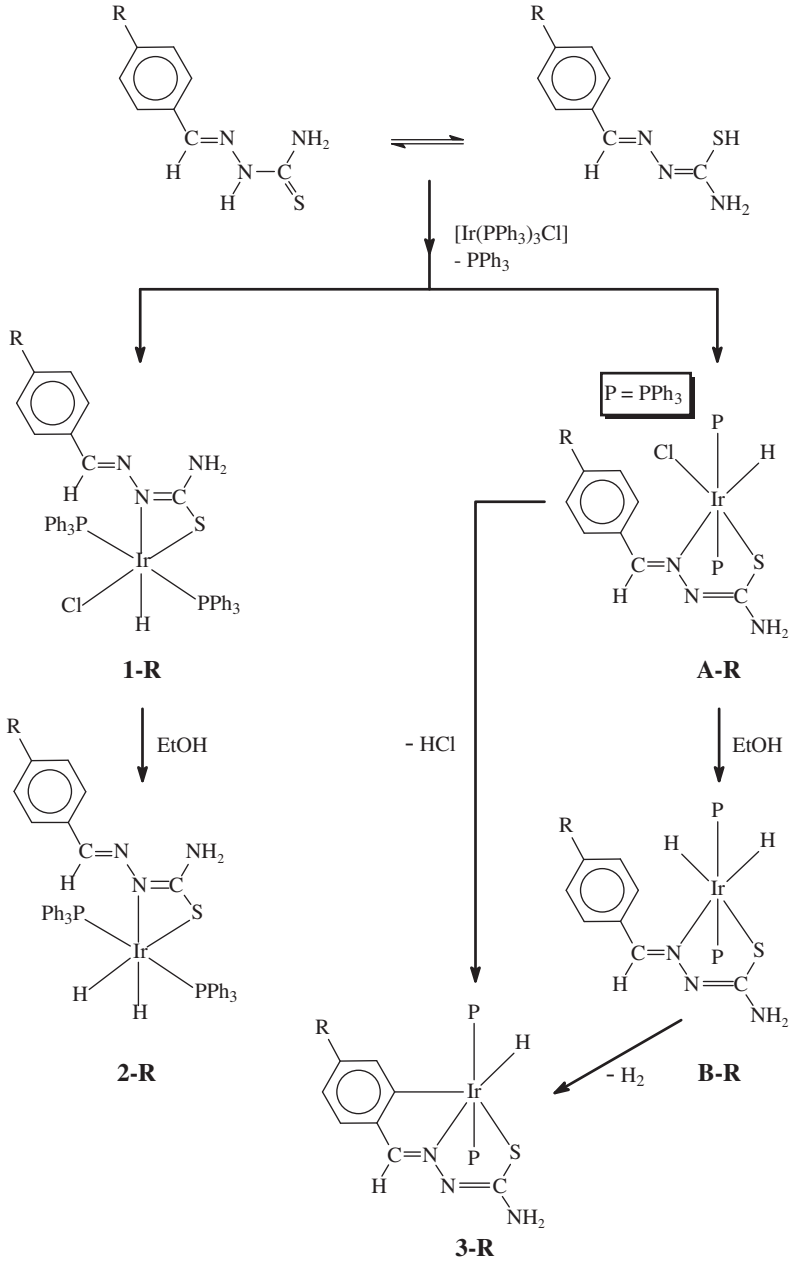

Scheme 1. Probable steps of the synthetic reaction in ethanol.

documented in the literature [14]. The **1-R** complexes for R≠NO_2 could not be isolated, probably because they undergo rapid irreversible conversion into the corresponding **2-R** (R≠NO_2) complexes in refluxing ethanol. In the other route, S–H bond activation takes place in the first step, as before, affording a mono-hydride intermediate A-R, where the thiosemicarbazone is coordinated to the metal center as a bidentate N,S-donor forming five-membered chelate ring (**III**). Hence each A-R intermediate is linkage isomer of the corresponding **1-R** complex. In alcoholic medium these A-R intermediates may convert into the corresponding dihydride species B-R, which are linkage isomers of the respective **2-R** complexes. In the final step, C–H activation at the ortho position of the pendant phenyl ring of the coordinated thiosemicarbazone (in B-R) takes place via molecular hydrogen leading to the formation of the **3-R** complexes [15]. The same **3-R** complexes may also be obtained from A-R via elimination of HCl. The hydride in **1-R**, as well as one of the two hydrides in **2-R**, is therefore generated from S-H activation by iridium, while source of the second hydride in **2-R** is ethanol. As isolated yield of the complex **2-R** (for R≠NO_2; or combined yield of **1-NO_2** and **2-NO_2** complexes) is found to be ~40% and that of complex **3-R** to be ~25%, it may be assumed that the **1-R** and A-R species, which are precursors of **2-R** and **3-R** complexes, respectively, are also formed in similar relative ratio irrespective of the nature of thiosemicarbazone ligands or, to be precise, with the nature of substituent R in the thiosemicarbazone ligands.

From the synthetic reactions carried out in toluene, organoiridium complexes of two types, viz. **3-R** and **4-R**, are obtained and the probable steps behind their formation are illustrated in Scheme 2. As before, oxidative insertion of iridium into the S–H bond of benzaldehyde thiosemicarbazone seems to take place in the initial step affording the intermediate A-R, as well as its geometric isomer C–R. It may be noted here that formation of **1-R**, the possible linkage isomer of A-R, has not been favored in refluxing toluene. Isomeri-

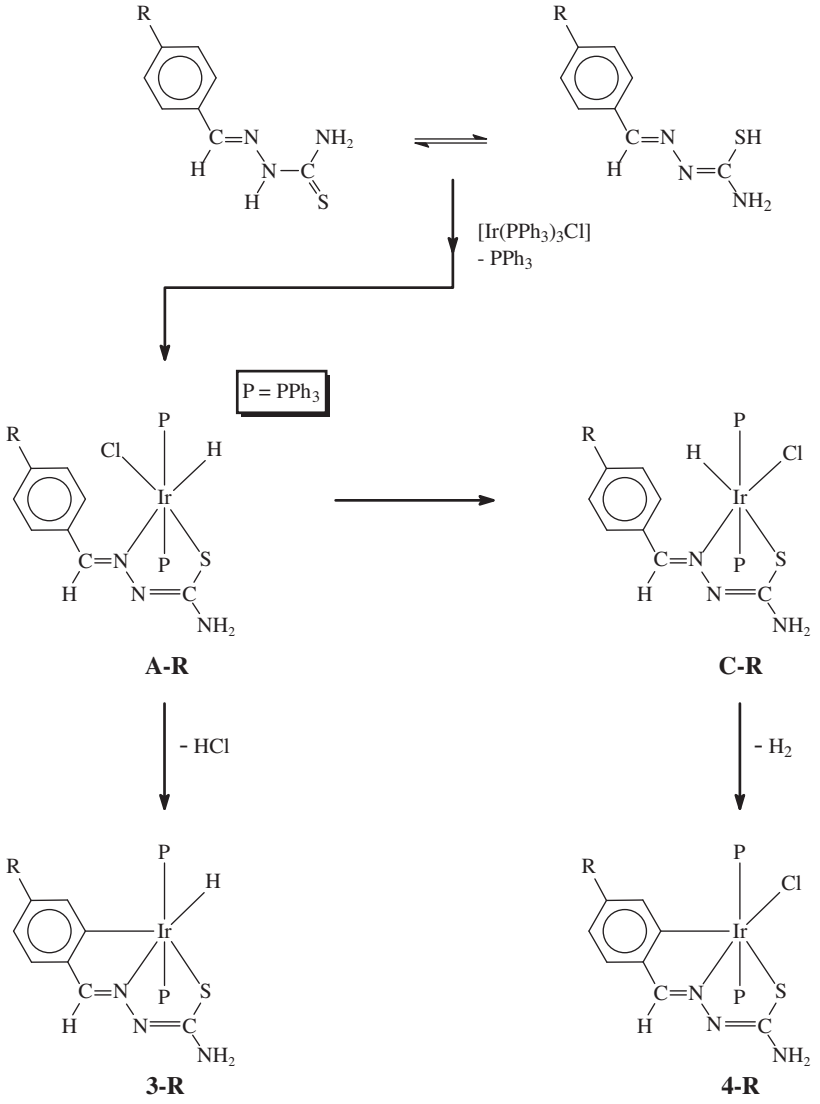

Scheme 2. Probable steps of the synthetic reaction in toluene.

zation of A-R into C-R in refluxing toluene, which did not take place in refluxing ethanol, is believed to be thermally driven. The intermediate A-R undergoes cyclometallation, via elimination of HCl, affording the **3-R** complex. Similarly complex **4-R** is obtained from the intermediate C-R through elimination of molecular hydrogen [15]. The speculated intermediates of these reactions could not be isolated, probably because they undergo rapid irreversible conversion into the corresponding cyclometallated species. In view of the observed yields of the **3-R** and **4-R** complexes, it appears that transformation of A-R into **3-R** and C-R takes place at comparable rates.

3.2. Spectral properties

Infrared spectra of the **2-R** ($R \neq NO_2$) and **3-R** complexes, respectively show two and one strong Ir–H stretch/stretches within 2097–2151 cm^{-1}. Three strong bands near 520, 695 and 745 cm^{-1} are observed in all these complexes due to the coordinated PPh_3 ligands. Several prominent bands are also displayed by these complexes within 1600–1000 cm^{-1}, which are absent in the spectrum of $[Ir(PPh_3)_3Cl]$, and hence these are attributable to the coordinated thiosemicarbazone ligands. Besides absence of the Ir-H stretch, infrared spectrum of each **4-R** complex is very similar to that of the corresponding **3-R** complex. ^1H NMR spectra of the **2-R** complexes show broad signals within 7.18–7.68 ppm due to the coordinated PPh_3 ligands. In each complex the two hydrides show two distinct signals near −15.0 and −20.0 ppm, which appear as doublet of triplets due to coupling with the two magnetically equivalent phosphorus nuclei as well as coupling between the two hydrides. Signal for the NH_2 fragment of the thiosemicarbazone is observed near 4.5 ppm. Most of the expected aromatic proton signals for the coordinated thiosemicarbazone ligand have been clearly observed, while few signals could not be detected due to their overlap with other signals. Signals for the hydrogen-containing substituents in the thiosemicarbazone ligand ($R = OCH_3$ and CH_3) are also observed in the expected region. ^1H NMR spectra of the **3-R** complexes show a hydride signal near −14.0 ppm, while the other spectral features are mostly similar to those of the **2-R** complexes. Besides absence of the hydride signal, ^1H NMR spectrum of any **4-R** complex is similar to that of the corresponding **3-R** complex. The infrared and ^1H NMR spectral data of all the complexes are therefore consistent with their composition and stereochemistry.

Electronic spectra of all the complexes have been recorded in acetonitrile solution. Each complex shows several intense absorptions in the visible and ultraviolet region (Table 3). The absorptions

Table 3
Electronic spectral and cyclic voltammetric data.

Compound	Electronic spectral data λ_{max}, nm (ε, M^{-1} cm^{-1})[a]	Cyclic voltammetric data[b] E, V vs. SCE
2-OCH$_3$	384(18000), 302(16600)[c], 254(28000)[c], 234(45000)[c]	1.33[d], 0.94[d], −1.26[e]
2-CH$_3$	386(14000), 302(14000)[c], 254(25900)[c], 234(45400)[c]	1.51[d], 0.94[d], −1.32[e]
2-H	388(15700), 306(18200)[c], 256(31200)[c], 234(54100)[c]	1.55[d], 0.95[d], −1.35[e]
2-Cl	392(9700), 306(12300)[c], 254 (22800)[c], 234(37400)[c]	1.57[d], 1.01[d], −1.37[e]
1-NO$_2$ + 2-NO$_2$	438(11100), 322(7500)[c], 270(16900)[c], 236(35800)[c]	1.45[d], 1.15[d], 0.71[d], −1.10[e], −1.50[e]
3-OCH$_3$	438(8100)[c], 276(40700), 236(75300)[c]	0.92[d], 0.43(77)[f], −1.28[e]
3-CH$_3$	436(3100), 264(27400)[c], 236(53200)[c]	1.14[d], 0.47(72)[f], −1.33[e]
3-H	438(6750), 274(32000)[c], 236(68500)[c]	1.16[d], 0.53(70)[f], −1.47[e]
3-Cl	451(2400), 268(24000)[c], 232(49400)[c]	1.26[d], 0.61(65)[f], −1.37[e]
3-NO$_2$	490(5200), 346(10100), 260(20300)	1.31[d], 0.78(70)[f], −0.74[e], −1.27[e]
4-OCH$_3$	450(4200), 342(3900)[c], 310(11800)[c], 274(29200)	1.09[d], 0.64(68)[f], −1.09[e]
4-CH$_3$	454(3500), 340(6300)[c], 310(11300)[c], 274(32000)	1.24[d], 0.66(76)[f], −1.06[e]
4-H	454(1800), 342(4500)[c], 312(7100)[c], 272(20700)	1.29[d], 0.73(61)[f], −1.04[e]
4-Cl	460(3400), 342(5400)[c], 312(11200)[c], 272(30500)	1.07[d], 0.79(70)[f], −1.05[e]
4-NO$_2$	532(3700), 382(6600)[c], 340(8100), 270(26700)	1.29[d], 0.92(73)[f], −1.0[e], -1.36[e]

[a] In acetonitrile.
[b] Solvent, acetonitrile; supporting electrolyte, TBAP; scan rate 50 mV s^{-1}.
[c] Shoulder.
[d] E_{pa} value.
[e] E_{pc} value.
[f] $E_{1/2}$ value (ΔE_p value), where $E_{1/2} = 0.5\ (E_{pa} + E_{pc})$ and $\Delta E_p = (E_{pa} - E_{pc})$.

in the ultraviolet region are attributable to transitions within the ligand orbitals. To have an insight into the nature of the absorptions in the visible region, qualitative EHMO calculations have been performed [16] on computer generated models of four representative members of the four types of complexes, where phenyl rings of the triphenylphosphines have been replaced by hydrogens. The results are found to be qualitatively similar for all the complexes. Compositions of selected molecular orbitals are given in Table 4 and partial MO diagram of a selected complex is shown in Fig. 5. Partial MO diagrams of the other complexes are deposited as supporting information (Figs. S1–S3). The highest occupied molecular orbital (HOMO) and the next two filled orbitals (HOMO-1 and HOMO-2) have major contributions from the iridium d_{xy}, d_{yz} and d_{zx} orbitals, and hence these three occupied orbitals may be regarded as the iridium t_2 orbitals. The lowest unoccupied molecular orbital (LUMO) has >85% contribution from the thiosemicarbazone ligand and is concentrated mostly on the imine (C=N) fragment. The LUMO+1 is localized on other parts of the thiosemicarbazone ligand. The lowest energy absorption in the visible region is therefore assignable to an allowed charge-transfer transition from the filled iridium t_2-orbital (HOMO) to the vacant π^*(imine)-orbital of the thiosemicarbazone ligand (LUMO). The other intense absorptions in the visible region may be assigned to charge-transfer transitions from the iridium t_2-orbitals to the higher energy vacant orbitals.

Table 4
Composition of selected molecular orbitals.

Compound	Contributing fragments[a]	% contribution of fragments to				
		HOMO	HOMO-1	HOMO-2	LUMO	LUMO+1
1-NO$_2$	Ir	85	78	77	0	0
	tsc-NO$_2$	10	17	17	98 (NO$_2$, 67)	98
2-H	Ir	82	79	79	0	0
	tsc-H	13	17	16	99 (C=N, 61)	100
3-H	Ir	72	44	63	9	0
	tsc-H	25	50	31	86 (C=N, 39)	91
4-H	Ir	75	44	63	10	0
	tsc-H	21	49	31	64 (C=N, 39)	94

[a] tsc-R means thiosemicarbazone ligand, where R is the substituent.

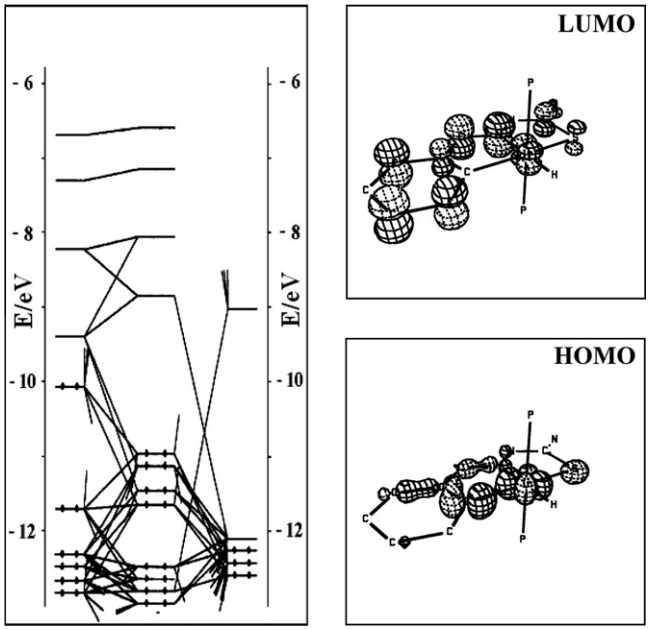

Fig. 5. Partial molecular orbital diagram of the **3-H** complex.

3.3. Electrochemical properties

Electrochemical properties of all the complexes have been studied by cyclic voltammetry in acetonitrile solution (0.1 M TBAP). Voltammetric data are given in Table 3. All the complexes show two oxidative responses on the positive side of SCE and a reductive response on the negative side. A representative cyclic voltammogram is deposited as supporting information (Fig. S4). In view of the composition of the HOMO, the first oxidative response is assigned to Ir(**III**)–Ir(**IV**) oxidation. The second oxidative response is tentatively assigned to oxidation of the coordinated thiosemicarbazone. In view of the composition of the LUMO, the reductive response is assigned to reduction of the coordinated thiosemicarbazone. One-electron stoichiometry of all the responses has been established by comparing their current heights with those of standard ferrocene/ferrocenium couple under identical experimental conditions. Except the Ir(**III**)–Ir(**IV**) oxidation in the **3-R** and **4-R** complexes, all the other redox responses are found to be irreversible. Potential of the irreversible redox responses did not show any systematic variation with the electron-withdrawing character of the substituent R in the thiosemicarbazone ligand. However,

potential of the reversible Ir(**III**)–Ir(**IV**) oxidation in the **3**-**R** and **4**-**R** complexes has been found to be sensitive to the nature of the substituent R. The potential increases with increasing electron-withdrawing character of the substituent R. The plots of oxidation potential versus σ [σ = Hammett constant of R [17]]; OCH_3 = −0.27, CH_3 = −0.17, H = 0.00, Cl = 0.23 and NO_2 = 0.78] are linear for both the $[Ir(PPh_3)_2(CNS\text{-}R)(H)]$ and $[Ir(PPh_3)_2(CNS\text{-}R)Cl]$ complexes (Figs. S5 and S6) with slopes (ρ) of 0.33 V and 0.27 V, respectively (ρ = reaction constant of this couple [18]). This shows that the *para*-substituent (R) on the thiosemicarbazone ligand, which is four-bonds away from the metal center, can still influence the metal-centered oxidation potential in a predictable manner.

4. Conclusions

The present study shows that $[Ir(PPh_3)_3Cl]$ can successfully mediate both S-H and C-H activation of the **4**-**R**-benzaldehyde thiosemicarbazones (**I**). However, the nature of complexes formed depends largely on the experimental factors. The present study also indicates that such bond activation of some other organic molecules, that have structural similarity with the benzaldehyde thiosemicarbazone, may be brought about by their reaction with $[Ir(PPh_3)_3Cl]$, and such possibilities are currently under exploration.

Acknowledgements

The authors thank the reviewers for their constructive comments, which have been helpful in preparing the revised manuscript. Financial assistance received from the UGC-CAS Program of the Department of Chemistry, Jadavpur University, is gratefully acknowledged. The authors thank the RSIC at Central Drug Research Institute, Lucknow, India, for the C, H, N analysis data, and the Department of Chemistry, Indian Institute of Technology, Kanpur, India, for the X-ray diffraction data of the **4**-$\mathbf{CH_3}$ complex.

Appendix A. Supplementary data

CCDC 761128, 761129 and 761130 contain the supplementary crystallographic data for this paper. These data can be obtained free of charge from The Cambridge Crystallographic Data Centre via www.ccdc.cam.ac.uk/data_request/cif. Supplementary data associated with this article can be found, in the online version, at doi:10.1016/j.ica.2010.04.009.

References

[1] (a) T.S. Lobana, R. Sharma, G. Bawa, S. Khanna, Coord. Chem. Rev. 253 (2009) 977;
(b) A.G. Quiroga, C.N. Raninger, Coord. Chem. Rev. 248 (2004) 119;
(c) J.R. Dilwarth, P. Amold, D. Morales, Y.L. Wong, Y. Zheng, Mod. Coord. Chem. (2002) 217;
(d) D.X. West, A.E. Liberta, S.B. Padhye, R.C. Chikate, P.B. Sonawane, A.S. Kumbhar, R.G. Yerande, Coord. Chem. Rev. 123 (1993) 49;
(e) D.X. West, S.B. Padhye, P.B. Sonawane, Struct. Bonding 76 (1992) 1;
[f] I. Haiduc, C. Silvestru, Coord. Chem. Rev. 99 (1990) 253;
(g) S.B. Padhye, G.B. Kaffman, Coord. Chem. Rev. 63 (1985) 127;
(h) M.J.M. Campbell, Coord. Chem. Rev. 15 (1975) 279.

[2] (a) A.C.F. Caires, Anticancer Agents Med. Chem. 7 (2007) 484;
(b) T. Wang, Z. Guo, Curr. Med. Chem. 13 (2006) 525;
(c) H. Beraldo, D. Gambino, Min. Rev. Med. Chem. 4 (2004) 31;
(d) E.M. Jouad, X.D. Thanh, G. Bouet, S. Bonneau, M.A. Khan, Anticancer Res. 22 (2002) 1713;
(e) M.B. Ferrari, F. Bisceglie, G. Pelosi, M. Sassi, P. Tarasconi, M. Cornia, S. Capacchi, R. Albertini, S. Pinelli, J. Inorg. Biochem. 90 (2002) 113;
(f) A.R. Cowly, J.R. Dilworth, P.S. Donnely, E. Labisbal, A. Sousa, J. Am. Chem. Soc. 124 (2002) 5270;
(g) R.I. Maurer, P.J. Blower, J.R. Dilworth, C.A. Reynolds, Y. Zheng, G.E.D. Mullen, J. Med. Chem. 45 (2002) 1420;
(h) J. Patole, S. Dutta, S.B. Padhye, E. Sinn, Inorg. Chim. Acta 318 (2001) 207;
(i) Z. Iakovidou, A. Papageorgiou, M.A. Demertzis, E. Mioglou, D. Mourelatos, A. Kotsis, P.N. Yadav, D. Kovala-Demertzi, Anticancer Drugs 12 (2001) 65.

[3] (a) S. Dutta, F. Basuli, A. Castineiras, S.M. Peng, G.H. Lee, S. Bhattacharya, Eur. J. Inorg. Chem. (2008) 4538;
(b) S. Halder, S.M. Peng, G.H. Lee, T. Chatterjee, A. Mukherjee, S. Dutta, U. Sanyal, S. Bhattacharya, New J. Chem. 32 (2008) 105;
(c) S. Halder, R.J. Butcher, S. Bhattacharya, Polyhedron 26 (2007) 2741;
(d) S. Basu, R. Acharyya, W.S. Sheldrick, H. Mayer-Figge, S. Bhattacharya, Struct. Chem. 18 (2007) 209;
(e) R. Acharyya, S. Dutta, F. Basuli, S.M. Peng, G.H. Lee, Larry R. Falvello, S. Bhattacharya, Inorg. Chem. 45 (2006) 1252;
(f) S. Dutta, F. Basuli, S.M. Peng, G.H. Lee, S. Bhattacharya, New J. Chem. 26 (2002) 1607;
(g) I. Pal, F. Basuli, T.C.W. Mak, S. Bhattacharya, Angew. Chem., Int. Ed. 40 (2001) 2923;
(h) F. Basuli, S.M. Peng, S. Bhattacharya, Inorg. Chem. 39 (2000) 1120;
(i) F. Basuli, M. Ruf, C.G. Pierpont, S. Bhattacharya, Inorg. Chem. 37 (1998) 6113;
(j) F. Basuli, S.M. Peng, S. Bhattacharya, Inorg. Chem. 36 (1997) 5645.

[4] (a) Y.P. Tian, C.Y. Duan, Z.L. Lu, X.Z. You, H.K. Fun, K. Sivakumar, Polyhedron 15 (1996) 2263;
(b) S. Halder, R. Acharyya, F. Basuli, S.M. Peng, G.H. Lee, S. Bhattacharya, unpublished results.

[5] (a) O. Daugulis, H.Q. Do, D. Shabashov, Acc. Chem. Res. 42 (2009) 1074;
(b) N.A. Foley, J.P. Lee, Z. Ke, T.B. Gunnoe, T.R. Cundari, Acc. Chem. Res. 42 (2009) 585;
(c) B.H. Lipshutz, Y. Yamamoto, Chem. Rev. 108 (2008) 2793;
(d) W. Leis, H.A. Mayer, W.C. Kaska, Coord. Chem. Rev. 252 (2008) 1787;
(e) J.C. Lewis, R.G. Bergman, J.A. Ellman, Acc. Chem. Res. 41 (2008) 1013;
(f) Y.J. Park, J.W. Park, C.H. Jun, Acc. Chem. Res. 41 (2008) 222;
(g) M. Lersch, M. Tilset, Chem. Rev. 105 (2005) 2471;
(h) E. Carmona, M. Paneque, L.L. Santos, V. Salazar, Coord. Chem. Rev. 249 (2005) 1729;
(i) T. Mallat, A. Baiker, Chem. Rev. 104 (2004) 3037;
(j) H.Y. Jang, M.J. Krische, Acc. Chem. Res. 37 (2004) 653.

[6] (a) S. Basu, I. Pal, R.J. Butcher, G. Rosair, S. Bhattacharya, J. Chem. Sci. 117 (2005) 167;
(b) R. Acharyya, F. Basuli, R.Z. Wang, T.C.W. Mak, S. Bhattacharya, Inorg. Chem. 43 (2004) 704.

[7] (a) D.T. Sawyer, J.L. Roberts Jr., Experimental Electrochemistry for Chemists, Wiley, New York, 1974;
(b) M. Walter, L. Ramaley, Anal. Chem. 45 (1973) 165.

[8] Chemical shifts are given in ppm and multiplicity of the signals along with the associated coupling constants (J in Hz) are given in parentheses. Overlapping signals are marked with an asterisk.

[9] G.M. Sheldrick, SHELXS-97 and SHELXL-97, Fortran programs for crystal structure solution and refinement, University of Gottingen, 1997.

[10] The first red product refers to the product obtained from evaporation of the first red fraction from the chromatography. Similarly the product obtained from evaporation of the second red fraction is referred to as the second red product.

[11] (a) G. Canepa, E. Sola, M. Martin, F.J. Lahoz, L.A. Ora, H. Werner, Organometallics 22 (2003) 2151;
(b) K.K.W. Lo, C.K. Chung, D.C.M. Ng, N. Zhu, New J. Chem. 26 (2002) 81;
(c) D.A. Ortmann, B. Weberndorfer, K. Ilg, M. Laubender, H. Werner, Organometallics 21 (2002) 2369;
(d) F. Torres, E. Sola, M. Martin, C. Ochs, G. Picazo, J.A. Lopez, F.J. Lahoz, L.A. Oro, Organometallics 20 (2001) 2716;
(e) H. Werner, A. Heohn, M. Schulz, Dalton Trans. (1991) 777.

[12] The first yellow product refers to the product obtained from evaporation of the first yellow fraction from the chromatography. Similarly the product obtained from evaporation of the second yellow fraction is referred to as the second yellow product.

[13] (a) D.A. Vicic, W.D. Jones, Organometallics 18 (1999) 134;
(b) R. McDonald, M. Cowie, Inorg. Chem. 32 (1993) 1671;
(c) L. Carlton, J.J. Molapisi, J. Organomet. Chem. 609 (2000) 60.

[14] (a) H.D. Empsall, S. Johnson, B.L. Shaw, Dalton Trans. (1980) 302;
(b) H.D. Empsall, E.M. Hyde, E. Mentzer, B.L. Shaw, M.F. Uttley, J. Chem. Soc. (A) (1976) 2069;
(c) J. Chatt, N.P. Johnson, B.L. Shaw, J. Chem. Soc. (A) (1964) 1625.

[15] The evolved hydrogen could not be detected.

[16] (a) C. Mealli, D.M. Proserpio, CACAO Version 4.0, Italy, 1994.;
(b) C. Mealli, D.M. Proserpio, J. Chem. Educ. 67 (1990) 399.

[17] L.P. Hammett, Physical Organic Chemistry, second ed., McGraw Hill, New York, 1970.

[18] R.N. Mukherjee, O.A. Rajan, A. Chakravorty, Inorg. Chem. 21 (1982) 785.